EASTERN SECTION
SEISMOLOGICAL
RESEARCH LETTERS

Are Ground-Motion Models Derived from Natural Events Applicable to the Estimation of Expected Motions for Induced Earthquakes?

by Gail M. Atkinson and Karen Assatourians

ABSTRACT

Natural earthquakes in western North America can be reasonable proxies for induced earthquakes in central and eastern North America because of the opposing effects that source depth and tectonic setting have on the stress parameter that scales high-frequency ground-motion amplitudes. It is critical that ground-motion prediction equations selected as induced-event proxies have appropriate near-distance scaling behavior for small-to-moderate shallow events. In this article, we describe the conditions under which natural-earthquake models are suitable for induced-seismicity applications. Using examples from Oklahoma and Alberta, we identify at least three models (Abrahamson *et al.*, 2014; Atkinson, 2015; Yenier and Atkinson, 2015b) that are reasonable proxy estimates of median motions from induced earthquakes in the east for the magnitude–distance range of most concern to hazard estimation from such events: **M** 3.5–6 at distances to 50 km.

INTRODUCTION

A key issue in the assessment of hazard from induced seismicity is the specification of ground-motion amplitudes associated with induced events, particularly at close distances (within tens of kilometers from the source). These are commonly estimated using ground-motion prediction equations (GMPEs) that express peak ground amplitudes and response spectra (PSA, 5% damped pseudospectral acceleration) as a function of moment magnitude (**M**), distance, and other variables. There is a paucity of well-calibrated and robust GMPEs derived strictly from induced events, although this situation is rapidly changing as new datasets become available. Therefore, induced-seismicity hazard applications have tended, of necessity, to draw on models of ground-motion amplitudes developed from natural events. This was the rationale for the Atkinson (2015; hereafter, A15) GMPE, which examined the magnitude and distance scaling for small-to-moderate events (**M** 3–6) at hypocentral distances (R_{hypo}) < 40 km. The A15 GMPE was derived from empirical analysis of natural events in California (the Next Generation Attenuation-West2 [NGA-W2] database; see Data and Resources). However, it explicitly addressed the point-source scaling attributes and near-distance saturation behavior expected for induced events, thus providing a middle ground between GMPEs developed entirely for natural events and GMPEs developed entirely for induced events.

The present article was motivated by an often-asked question: Is the A15 GMPE applicable for estimation of motions from induced events in central and eastern North America (CENA)? And if so, why? This is a good question, because the A15 GMPE was derived from natural events, which have on average a deeper focus than most induced events. Moreover, there may be differences in ground-motion characteristics between natural and induced events. Finally, the events used to develop the A15 model occurred in California rather than CENA. Thus, there are three potential reasons that the A15 GMPE may not be applicable (depth, natural vs. induced characteristics, tectonic setting). Fortuitously, the effects of depth and tectonic setting tend to offset each other, as will be shown in this article. Moreover, recent information suggests that, for the same focal depth and tectonic setting, the ground motions for natural and induced events appear to be similar (Yenier and Atkinson, 2015b). Taken together, these factors suggest that California events having depths of 6–10 km should be reasonable proxies for CENA events (regardless of whether they are natural or induced) having depths of 2–6 km. The veracity of this claim is demonstrated using a database of induced-event ground motions for **M** ≥ 3.8 at distances < 50 km (Assatourians and Atkinson, 2017; see Data and Resources).

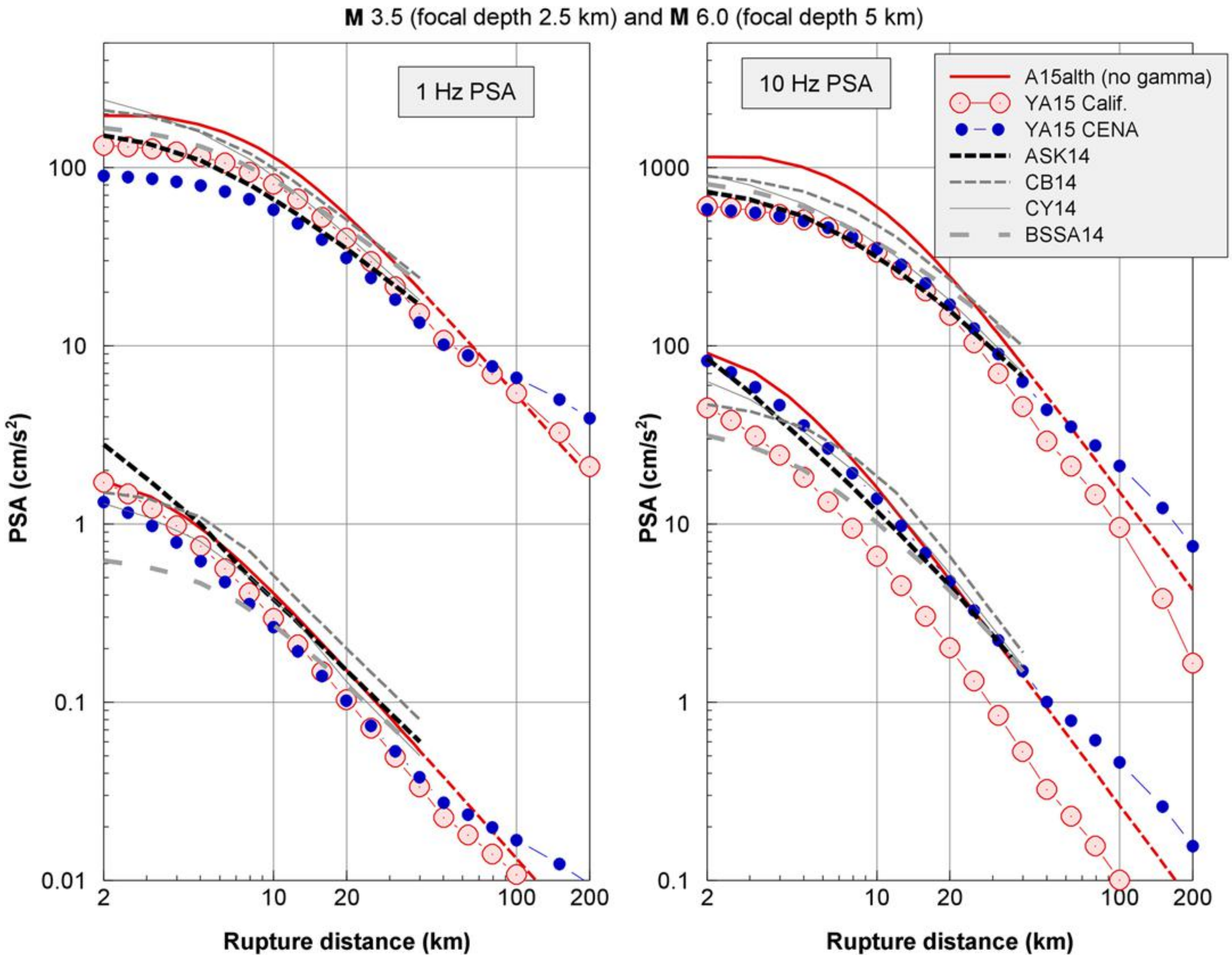

▲ **Figure 1.** Comparison of empirical ground-motion prediction equations (GMPEs) developed from Next Generation Attenuation-West2 (NGA-W2) data with Yenier and Atkinson (2015b; hereafter, YA15) equivalent point-source model GMPE for California and CENA (calibrated to NGA-W2 and NGA-East, respectively, as described in Yenier and Atkinson, 2015b). Assumed focal depth is 2.5 km for **M** 3.5, 5 km for **M** 6. The median stress values for these focal depths in the YA15 model are 2 bars (California), 19 bars (CENA) for **M** 3.5 and 58 bars (California), 70 bars (CENA) for **M** 6.0. NGA-W2 models are evaluated assuming that the depth to the top of rupture is unknown. All models are applicable to the geomean horizontal component (or equivalent) for a reference B/C site condition. The color version of this figure is available only in the electronic edition.

We also identify two other natural-earthquake GMPEs that can be used for induced-seismicity applications in CENA, and explain why. Natural earthquakes in western North America can be reasonable proxies for induced earthquakes in CENA because of the opposing effects that source depth and tectonic setting have on the stress parameter, which controls high-frequency ground motion. But not all GMPEs are suitable for this application. It is critical that GMPEs selected as induced-event proxies have appropriate near-distance ($R_{hypo} < 10$ km) scaling behavior for small-to-moderate shallow events. The A15 GMPE is a good proxy because it was developed explicitly to model the near-distance scaling attributes expected for induced events. Of the suite of NGA-W2 GMPEs, none are explicitly considered to be for induced events. However, the Abrahamson *et al.* (2014) GMPE model is a good proxy for induced events in CENA due to attributes of its functional form. In contrast, the other NGA-W2 GMPEs (Boore *et al.*, 2014; Campbell and Bozorgnia, 2014; Chiou and Youngs, 2014) use functional forms that are not well suited for induced-seismicity applications. Of recent GMPEs developed for CENA, those that explicitly consider focal depth as a source parameter and which have appropriate near-distance saturation for small-to-moderate events are potentially applicable. An example is the Yenier and Atkinson (2015b; hereafter, YA15 CENA) GMPE model developed with the NGA-East (NGA-E) database.

KEY SCALING ATTRIBUTES OF GMPES FOR APPLICABILITY TO INDUCED EVENTS IN CENA

Figure 1 shows key scaling attributes of selected GMPEs for the magnitude range of most interest for induced-seismicity hazard assessment, **M** 3.5–6.0 (e.g., Atkinson *et al.*, 2015; Bourne *et al.*, 2015). All GMPEs are giving the 5% damped PSA for the geomean horizontal component (or equivalent), for a reference National Earthquake Hazards Reduction Program (NEHRP) site condition of B/C (time-averaged shear-wave velocity in the top 30 m of $V_{S30} = 760$ m/s). It is interesting to compare the A15 GMPE, which is an empirical model developed from California data, with the simulation-based YA15 models for California and CENA. The A15 model originally considered two alternatives for the term in the functional form that controls near-distance saturation scaling. It has since been determined, using additional data, that of the two considered saturation models, the one called the alternative-*h* model is more appropriate (Atkinson *et al.*, 2016). This model features a saturation distance (*h*) that increases from a value of 2.4 km at **M** 3.5 to a value of 7.2 km at **M** 6. It is this saturation term that causes the A15 curves of Figure 1 to approach near-constant amplitudes at distances closer than these values. We adopt the alternative-*h* version of A15 for this article, but this choice is not critical. Other NGA-W2 GMPEs are also shown in Figure 1 for reference.

The comparison of empirical GMPEs with YA15 in Figure 1 is useful because the YA15 models are based on an equivalent-point-source parameterization, thereby allowing the underlying seismological model parameters of the A15 (or other) GMPEs to be inferred. The YA15 models (Yenier and Atkinson, 2015b) were calibrated using the NGA-W2 database for California and the NGA-E database for CENA (see Data and Resources). The key source parameters in the YA15 models are seismic moment and the stress parameter. The seismic moment controls the low-frequency level of the spectrum. The stress parameter is essentially a marker for the best corner frequency by which to characterize the response spectrum at near-source distances, in the context of the Brune single-corner omega-squared point-source stochastic model (for details, see Boore, 2003; Yenier and Atkinson, 2015b). The stress parameter controls the relative balance of high-frequency to low-frequency amplitudes in this model representation. Note that the stress parameter is so called because it has units of stress, but we do not credit it with any physical meaning; it is simply a model parameter that reflects the observed spectral corner. Figure 2 illustrates the effect of the stress parameter on spectral amplitudes and shape, using as an example an event of **M** 4.0 at a distance of 8.5 km from the hypocenter, as evaluated using the YA15 CENA model. Available records from Oklahoma for this magnitude value (see Data and Resources), in the distance range of from 7 to 10 km, are shown for a sample comparison with the model amplitudes; no fitting is implied, it is a simple comparison. The data used, and their correction to equivalent values for B/C site conditions, are discussed later. It can be seen from Figure 2 that larger spectral amplitudes at high frequencies, relative to those at low frequencies, imply higher values of the stress parameter in the YA15 model.

Yenier and Atkinson (2015a,b) showed that the value of stress parameter that best describes the spectral amplitude data increases with focal depth in both California and CENA. It has been pointed out (Chris Cramer, personal comm., 2016) that the depth dependency may be at least partly due to enhanced contributions of surface waves to low-frequency amplitudes for shallow events. Moreover, we do not attempt to build depth dependence of shear-wave velocity into the equation that converts corner frequency to stress, to avoid unnecessary complications and sensitivities in the interpretation of the stress values —and because focal depth is often a poorly known parameter. Instead, we reference all conversions of corner frequency to stress parameter using a fixed shear-wave velocity of 3.7 km/s, which is applicable for midcrustal depths. These factors may explain at least in part why the stress parameter values increase steeply with increasing focal depth.

The stress parameter increases with magnitude, in addition to its dependence on depth, but becomes a constant for **M** >~4.5. The scaling behavior of the stress parameter with magnitude and depth is similar for California and CENA, but the values of stress are systematically higher in CENA in comparison with those of California events (for the same magnitude and depth). The effect of the higher stress parameter in CENA becomes most apparent at natural-earthquake depths;

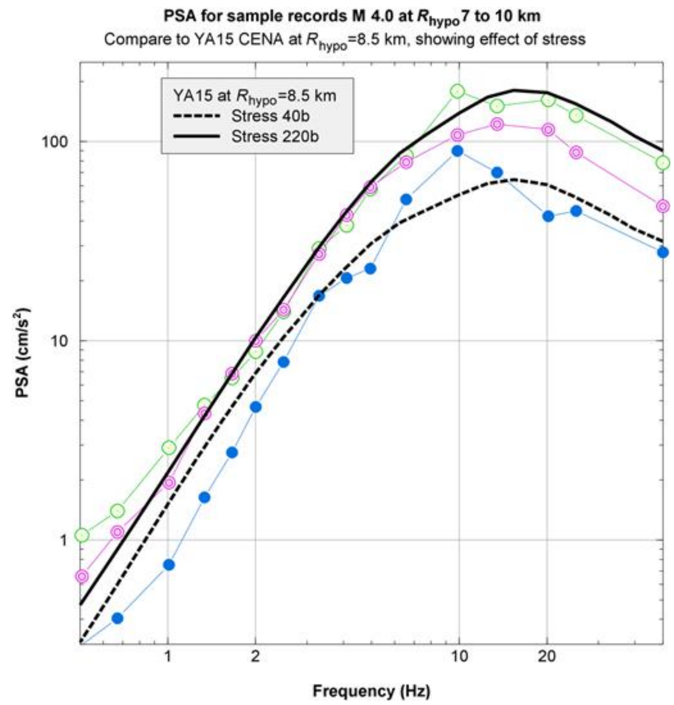

▲ **Figure 2.** The effect of stress parameter on spectral shapes and amplitudes in the YA15 model (Yenier and Atkinson, 2015b). Response spectra are shown for an **M** 4 event at $R_{hypo} = 8.5$ km for stress parameter values of 40 bars (dashed line) and 220 bars (solid line), for the YA15 central and eastern North America (CENA) GMPE equations (B/C site conditions). Observed spectra for **M** 4.0 records in Oklahoma having 7 km ≤ R_{hypo} ≤ 10 km are shown to illustrate typical comparisons of model to recorded data (lines with dots; from top to bottom, the events are those recorded on 10 April 2014, 20 June 2015, and 25 September 2015). The color version of this figure is available only in the electronic edition.

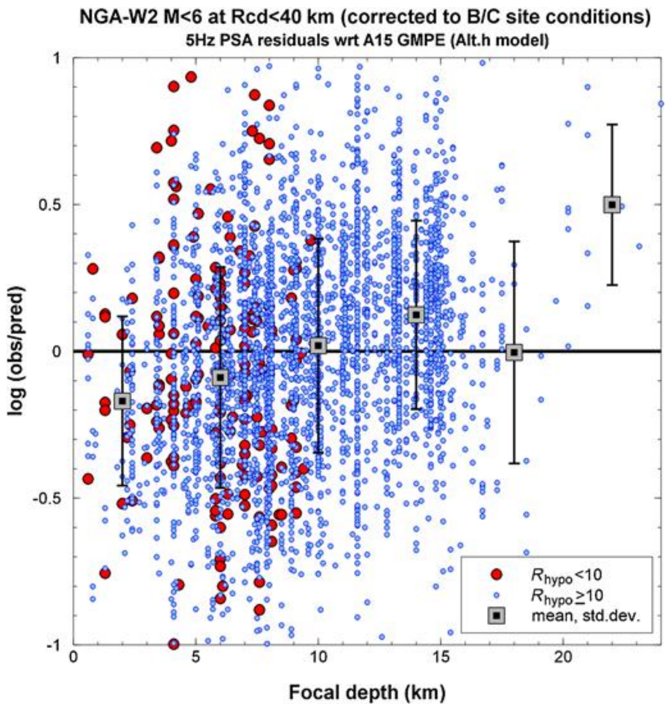

▲ **Figure 3.** Residuals of Atkinson (2015; hereafter, A15) GMPE versus focal depth (for NGA-W2 data, corrected to B/C site conditions). Squares with error bars are mean and standard deviation in focal depth bins of 4 km width. Larger circles show data points at hypocentral distances <10 km; smaller circles show data points for hypocentral distances of 10–40 km. The color version of this figure is available only in the electronic edition.

for shallow events, the effect is obscured by the steep scaling of the stress parameter value with focal depth. Based on a limited sample of induced and very shallow natural events, Yenier and Atkinson (2015b) and Yenier *et al.* (2017) found no compelling evidence that the value or scaling of the stress parameter for induced CENA events differs from that of natural events. The behavior of the stress parameter with depth and magnitude is illustrated later in the article (see Fig. 5).

In the GMPE comparisons of Figure 1, it is assumed that the depth of the hypocenter is 2.5 km for the **M** 3.5 event and 5 km for the **M** 6.0 event in plotting the A15 and YA15 models. An interesting observation is that the CENA and California curves are very similar for **M** 6 at 10 Hz for the YA15 models. This is because the stress parameter values for CENA and California are nearly the same for this magnitude and depth. In contrast, at natural event depths, the stress parameter attains a value that is about a factor of 3 higher in CENA than in California. It is assumed in evaluating the NGA-W2 models (using the spreadsheet noted in Data and Resources) that the depth to the top of the rupture is unknown. For the assumed depths, the rupture should nearly reach the surface, but the assumption of an unknown depth is used to make all NGA-W2 GMPEs consistent (depth to top of rupture or focal depth is not included in all models). Moreover, using an unspecified depth to top of rupture in the NGA-W2 models has the effect of assuming typical focal depths for all events; the rationale for this choice will become apparent in later discussion.

Most GMPEs use closest distance to the fault rupture surface (D_{rup}) as the distance metric. The A15 GMPE uses hypocentral distance R_{hypo} because D_{rup} is generally not well defined for induced events, and R_{hypo} is a convenient measure for point-source scaling. For plotting purposes in Figure 1, R_{hypo} has been converted to the equivalent value of D_{rup}, assuming a vertical fault that nearly touches the surface. The NGA-W2 GMPEs are shown in Figure 1 to a distance of 40 km to emphasize near-distance scaling differences. The Abrahamson *et al.* (2014; hereafter, ASK14), Campbell and Bozorgnia (2014; hereafter, CB14), and Chiou and Youngs (2014; hereafter, CY14) GMPEs use D_{rup} as the distance metric, whereas Boore *et al.* (2014; hereafter, BSSA14) use closest distance to the surface projection of the rupture (R_{JB}). The BSSA14 GMPE is easily converted to D_{rup} in Figure 1 because $D_{rup} = R_{JB}$ for the assumed geometry.

A key attribute of the scaling in Figure 1 is the near-distance saturation of ground-motion amplitudes. This is controlled by the functional form in GMPEs because data have not been available to empirically constrain this shape until very recently. Point-source scaling concepts suggest that events of **M** 3.5 should not have significant near-distance saturation. This has recently been confirmed by analysis of empirical data from induced events in the Geysers, California, region (Atkinson *et al.*, 2016) and in Oklahoma (Yenier *et al.*, 2017); these recent analyses support the alternative-*h* saturation shape in A15.

It is observed in Figure 1 that most of the NGA-W2 GMPEs do not have sufficient magnitude dependence of the near-distance scaling shape to match the behavior expected from equivalent point-source modeling concepts for small-to-moderate-induced events. An exception is the ASK14 GMPE, which follows the expected near-distance saturation well (e.g., as given in YA15 and A15). This is because the ASK14 GMPE explicitly considered the appropriate magnitude scaling of this term, based on seismological concepts. In contrast, the BSSA14 GMPE is not a good proxy for induced events because the R_{JB} metric does not allow for the handling of focal depth effects that are critical for shallow events.

An interesting issue that arises is that the A15 GMPE did not include focal depth as an explicit parameter; depth enters the A15 model only indirectly, through the use of R_{hypo} as the distance metric. This means that the A15 GMPE implicitly applies to events having average focal depth. For the California events of **M** 3–6 used in the A15 development, this means that the average depth of events to which the GMPE applies is ~8 km. The unmodeled focal depth effects will map into residual effects, in which residuals are defined as the log(base10) of the ratio between observed and predicted amplitudes. These effects can be seen in Figure 3, which plots residuals (for PSA at 5 Hz) as a function of focal depth (d) for the A15 GMPE. It is noted that residuals tend to be negative for shallow events ($d < 10$) and positive for deep events ($d > 10$), while being neutral for events of near-average depth. These residual trends are attributable to the dependence of the stress parameter on focal depth. Shallow events tend to have low stress parameters, and thus negative residuals at high frequencies, whereas deep events have high-stress parameters and positive high-frequency ground-motion residuals.

The negative residuals with respect to A15 for shallow events suggest that A15 may be conservative when applied to induced events. On the other hand, the effect of focal depth on the stress parameter (and hence on high-frequency ground motion) is not the only source effect that needs to be considered. A counterbalancing effect is that stress parameters in California tend to be lower than those in CENA. If we are predicting motions for induced events in CENA, this factor also needs to be taken into account.

The YA15 generic GMPE is based on a calibrated equivalent-point-source model, which provides a convenient tool with which to explore the influence of the stress parameter on GMPE models (for a review of the stochastic point-source model, see Boore, 2003). The YA15 GMPE comprises a linear combination of source, path, and site terms that are easily separated:

$$\ln Y = F_E + F_Z + F_\gamma + F_S + C \quad (1)$$

(Yenier and Atkinson, 2015b), in which $\ln Y$ is the natural logarithm of a ground-motion intensity measure, such as the PSA at a selected frequency. F_E, F_Z, F_γ, and F_S represent functions for earthquake source, geometrical spreading, anelastic attenuation, and site effects, respectively. The earthquake source term is based on an equivalent Brune point-source model, whereas the attenuation terms are determined empirically (for details, see Boore, 2003). The C term is a frequency-dependent empirical calibration factor that accounts for the average residual differences between simulations and empirical data. The C term accounts for unmodeled effects, including the contributions of surface waves to longer period motions, and any residual site effects not accounted for in the site-effects model. These effects vary regionally and thus the calibration term for CENA differs from that for California; both are implemented here as described in Yenier and Atkinson (2015b). In the original Yenier and Atkinson (2015a) GMPE for California, this term was defined as a constant designed primarily to model long-period residuals; in Yenier and Atkinson (2015b), the calibration constant was refined to include a frequency dependence so that it could model a mixture of effects.

The source function (F_E) describes the effects of magnitude and stress parameter on ground-motion amplitudes. Within this function, the effects of magnitude and stress parameter on amplitudes have been decoupled:

$$F_E = F_M + F_{\Delta\sigma} \quad (2)$$

in which F_M represents the magnitude effect on ground-motion amplitudes that would be observed at the source, if there were no near-distance-saturation effects. Near-distance saturation is handled by the use of an equivalent-point-source distance metric in the geometric spreading function:

$$R = \sqrt{D_{\mathrm{rup}}^2 + h^2} \quad (3)$$

in which D_{rup} is the closest distance from the site to the fault-rupture surface and h is a pseudodepth term that accounts for distance saturation effects. The pseudodepth term is adopted from inversion results for active regions (Yenier and Atkinson, 2015a), for which there are sufficient data to constrain such effects:

$$h = 10^{-0.405+0.235\mathbf{M}}. \quad (4)$$

The h term is what controls the near-source saturation behavior and its scaling with magnitude, forcing the GMPE curves to approach near-constant values at very close distances, as seen in Figure 1. The alternative-h saturation model assumed by A15 is very similar to that given by equation (4). Both have a value of $h = 2$ km for **M** 3. The A15 model is slightly less steep in its increase of h with magnitude: the YA15 saturation term attains a value of $h = 10$ km for **M** 6, whereas the A15 term attains a value of $h = 7.2$ km for **M** 6. It is this magnitude-dependent behavior of the near-distance scaling term that is critical for GMPEs for small-to-moderate events at close hypocentral distances, since this term will control the maximum amplitudes that the GMPE can attain as the source is approached.

The YA15 CENA GMPE is defined for a reference stress ($\Delta\sigma$), κ_0 parameter (representing near-surface attenuation), and site condition; the use of a reference stress shifts the effects of stress parameter into a separate term ($F_{\Delta\sigma}$). This simplifies the modification of the GMPE for alternative values of stress ($\Delta\sigma$), and also facilitates the evaluation of event-specific values of stress, without the need to repeat simulations.

Yenier and Atkinson (2015b) used the generic GMPE formulation to evaluate the value of stress within this framework for each event, using the NGA-W2 database for California events and the NGA-E database for CENA events. For each region, they developed a median stress model to fit the observations. In both regions, the value of the stress parameter is observed to increase with magnitude for small events, then attain a constant value for events of $\mathbf{M} > \sim 4.5$. In both regions, the stress parameter increases significantly with increasing focal depth. This explains the residual trend seen in Figure 3 because the A15 GMPE did not include focal depth as a predictive variable and thus did not model its effect on high-frequency ground-motion amplitudes. Although the nature of the trends in the stress parameter is similar in California and CENA, there is an important difference: the value of stress is systematically higher in CENA than in California. This difference in average stress in midplate versus active regions is well known from many previous studies dating back to the 1970s (e.g., Kanamori and Anderson, 1975). Yenier and Atkinson (2015b) had both natural and induced events within the CENA database. Natural events will tend to have higher stress values because they are deeper, but no difference in stress for natural versus induced events was observed for events of similar focal depth.

The YA15 generic GMPE can be easily evaluated with a specified stress parameter (rather than using the median value

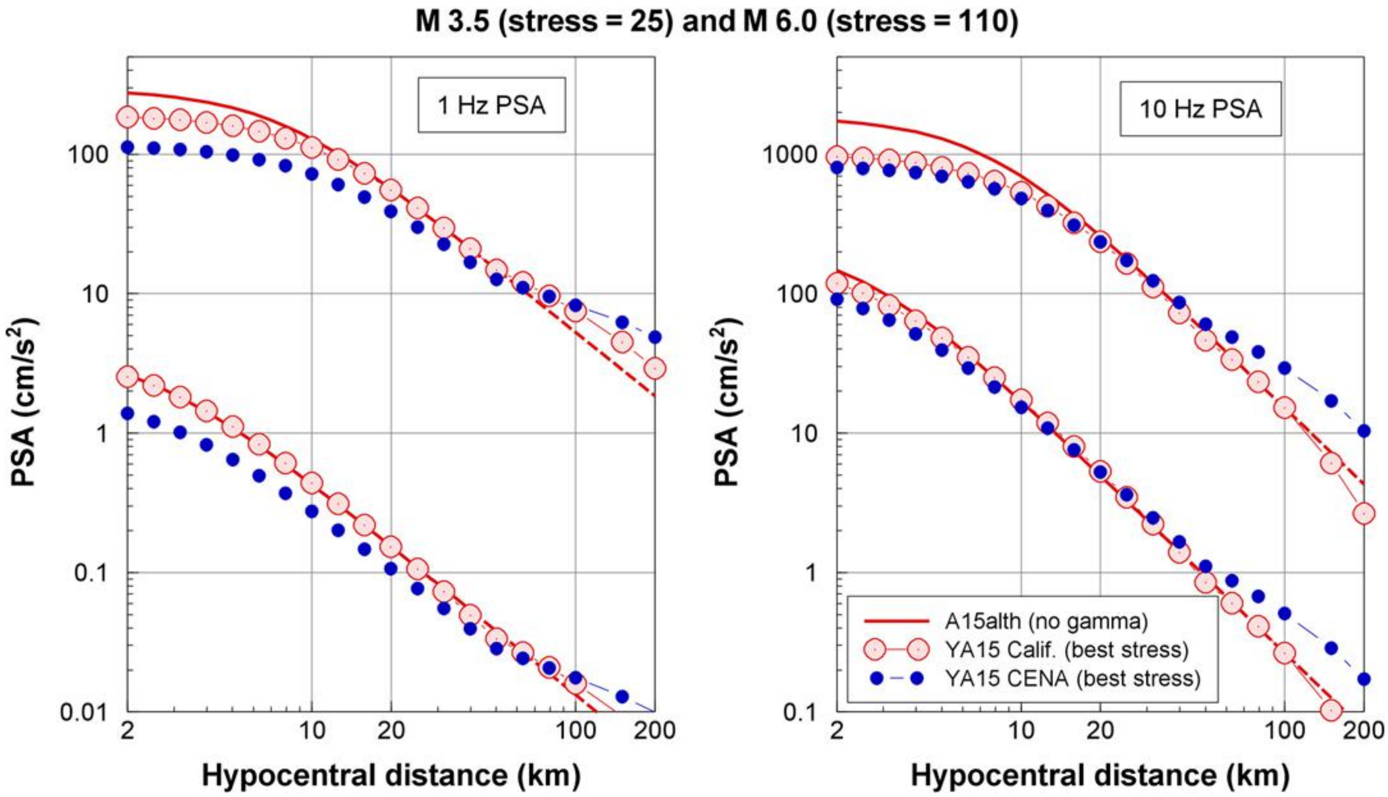

▲ **Figure 4.** Comparison of A15 empirical GMPE (alternative saturation, no added anelastic term) with YA15 equivalent point-source-model GMPEs for California and CENA, for **M** 3.5 and 6.0, with YA15 stress level chosen to match A15 at each magnitude (25 bars for **M** 3.5, 110 bars for **M** 6.0). The color version of this figure is available only in the electronic edition.

corresponding to a given magnitude and focal depth), using the $F_{\Delta\sigma}$ term in equation (2). We use this feature to determine, by inspection, the approximate value of stress parameter implied by the A15 GMPE. This is illustrated in Figure 4, in which we compare the A15 GMPE (alt-*h* saturation) for **M** 3.5 and 6.0 with the YA15 model GMPE for both the California and CENA attenuation rates, choosing to plot YA15 for the value of stress parameter that best matches the level of the A15 GMPE in the hypocentral distance range from ~10 to 20 km (in which data are most plentiful). Because of the specification of a fixed stress value, the California and CENA curves are very similar except at large distances, for which the slower anelastic attenuation in CENA becomes important. In Figure 4, the A15 GMPE is plotted without any added anelastic term (i.e., c4 = 0); in plotting YA15, it is assumed that $R_{\rm hypo} \sim D_{\rm rup}$. The level of the YA15 curves is sensitive to the value of stress at high frequencies, but insensitive at lower frequencies. By inspection, we infer that if we specify a value of 25 bars for stress for **M** 3.5 and 110 bars for stress for **M** 6.0, the A15 GMPE closely follows the equivalent point-source model curves of YA15.

We can repeat the exercise shown in Figure 4 for **M** 3.0, 3.5, ..., 7.0, comparing the A15 GMPE for frequencies from 1 to 10 Hz with the YA15 model curves for different values of stress. The value of stress parameter implied by the A15 GMPE is shown as a function of magnitude in Figure 5, in comparison with the values of stress determined by YA15 for events in both California and CENA. The use of the A15 GMPE for **M** > 6 is an extrapolation, but the implied stress parameter nevertheless appears reasonable. The YA15 median models for stress in both regions are also shown. The value of stress parameter implied by A15 is consistent with the observed values for California events having focal depths in the range from 5 to 10 km. This is as we would expect. The noteworthy feature of Figure 5 is that the average stress parameter implied by the A15 GMPE is consistent with the observed values of the stress parameter for very shallow CENA events with focal depths less than 5 km. Figure 5 implies that the effect of shallow focal depth on the value of the stress parameter is approximately offset by the systematic difference between CENA and California. This is why the A15 GMPE should be a reasonable proxy for an induced-event GMPE for CENA.

It also follows from this logic, and from Figure 1, that the Abrahamson *et al.* (2014) NGA-W2 GMPE should be a reasonable proxy for induced events in CENA, but only if the depth to the top of rupture is specified as unknown when evaluating the GMPE. The reason for this proviso is that the depth to the top of rupture is essentially a focal depth parameter that carries an implied stress parameter scaling. If a near-surface rupture depth is specified in Abrahamson *et al.* (2014), the high-frequency ground motions will scale down to reflect a shallow event having a lower value of stress parameter; this is

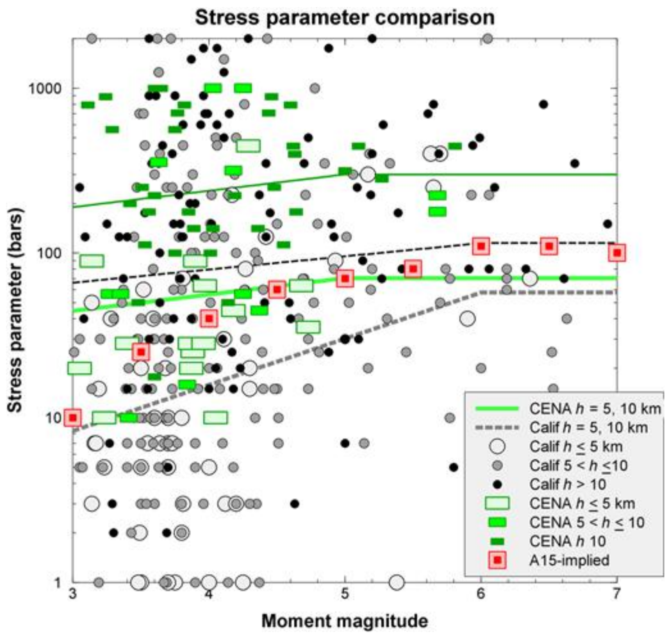

▲ **Figure 5.** Inferred stress parameter as a function of magnitude for A15 GMPE (squares) compared with empirical stress data (symbols) and models (lines) of YA15 for California and CENA. Circles are stress values from YA15 for events in California (from Yenier and Atkinson, 2015a); rectangles are stress values from YA15 for events in CENA (Yenier and Atkinson, 2015b) (both coded by focal depth). Lines show median stress model of YA15 for California (dashed) and CENA (solid) for focal depths of 5 and 10 km. The color version of this figure is available only in the electronic edition.

appropriate for California, but not for induced events in CENA. Specification of an unknown depth to top of rupture (within the spreadsheet algorithm referenced in Data and Resources) has the effect of forcing the Abrahamson *et al.* (2014) depth to top of rupture to correspond to that expected for an event of average depth in California—which results in ground motions that are reasonable for shallow events in CENA (Fig. 5). Thus, the specification of an event of average depth (or equivalently an event with unknown depth to top of rupture) can be used to manipulate the ASK14 GMPE into predicting ground motions having appropriate spectral levels for induced events in CENA.

Use of A15 (or ASK14) as a proxy for induced events in CENA ignores attenuation effects, which are known to be slower in CENA than in California. Thus, some caution is required, in that we must acknowledge that amplitudes will be underestimated as distance increases when using California GMPEs as CENA induced-event proxies. From Figures 1 and 4, it is apparent that these effects become important at distances greater than 40 km. However, for the small-to-moderate events of most concern to induced-seismicity hazard in low-seismicity regions (e.g., Bourne *et al.*, 2015), almost all hazard contributions will come from distances that are less than 40 km, and thus this shortcoming is of limited practical consequence.

Finally, the YA15 CENA GMPE is appropriate for application to induced events, because the dependence of stress on focal depth in CENA, which applies to both natural and induced events, is explicitly modeled. Moreover, the YA15 CENA model explicitly uses CENA attenuation and thus decays appropriately to distances of hundreds of kilometers.

ILLUSTRATION FOR RECENT INDUCED EVENTS IN CENA

In the previous section, we described why at least three published GMPEs developed using natural earthquakes should be reasonable proxies for induced earthquakes in CENA: these are the ASK14 NGA-W2 GMPE with the specification of an unknown depth to the top of rupture (regardless of the actual depth), the A15 GMPE (in which focal depth is not a specified parameter), and the YA15 GMPE for CENA (using an appropriate shallow focal depth for induced events). In this section, we demonstrate that these proxies are a reasonable first-order description of induced-event amplitudes for events of $\mathbf{M} \geq 3.8$ recorded at close distances in Oklahoma and Alberta. To do this, we use a database compiled by Assatourians and Atkinson (2017). The purpose of that database is to provide spectral amplitudes and processed time histories for those induced events of most engineering interest; the database comprises publicly available broadband and accelerometer records from events in Oklahoma and Alberta from 2010 to 2016 at distances < 20 km for **M** 3.8–4.5 and at distances to 50 km for $\mathbf{M} \geq 4.5$ (see Data and Resources). It should be noted that this database, composed of a few hundred records, is not intended to be a spectral amplitude database for GMPE development for induced events. For broader GMPE development purposes, a larger compilation project is required. GMPE development for induced events requires thousands of records over a broad distance range, so that the effects of source, path, and site can be separated empirically; this larger database compilation is in progress. There is also an NGA project for induced seismicity underway at Pacific Earthquake Engineering Research Center (PEER) that will compile a suitable database. While these larger projects are being conducted, we use the targeted database of Assatourians and Atkinson (2017) to display a comparison between key observations and the GMPEs suggested as interim induced-event proxies.

In Figure 6, the GMPEs are compared with recorded horizontal-component (geomean) ground motions from events of **M** 4.0–4.5 in Oklahoma and Alberta. The site conditions of the recording stations are not yet classified in available databases. To make an approximate correction to the B/C reference condition of the GMPEs, it is assumed that all records are on NEHRP site class C, with $V_{S30} = 450$ m/s. The site correction factors of Seyhan and Stewart (2014), assuming linear site response, are used to make a first-order correction from C to B/C. The assumption of class C is likely a reasonable average when taken over the database, but is not intended to represent a realistic site correction for any individual record. The use of an average site correction factor will map into increased variability

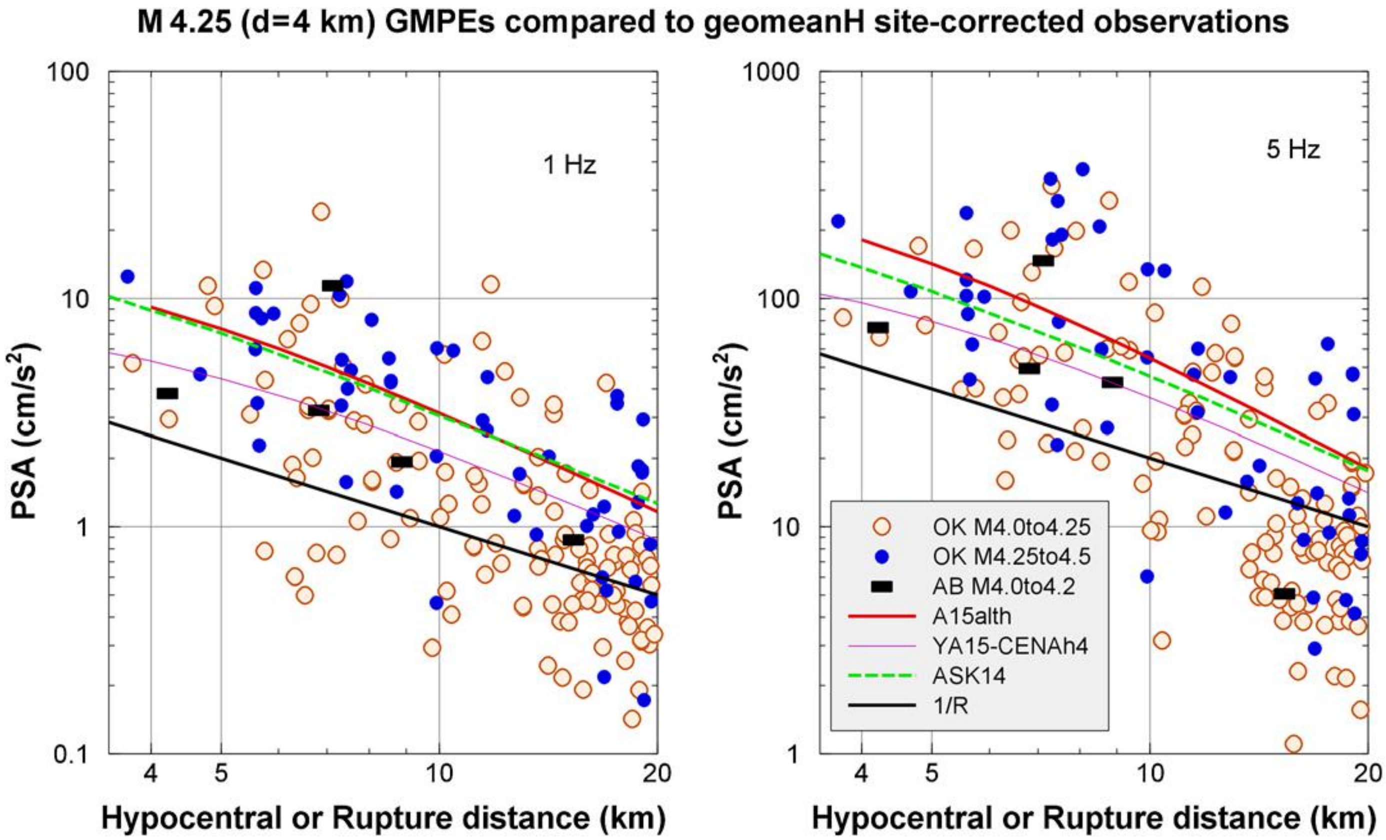

▲ **Figure 6.** Observed horizontal-component ground motions (symbols) for induced events of **M** 4.0–4.5 (converted to B/C) in Oklahoma (OK) and Alberta (AB), compared with A15 (alternative-*h* model), YA15 CENA (assumed depth = 4 km), and Abrahamson *et al.* (2014, hereafter, ASK14) (unspecified depth) GMPEs (lines). ASK14 and YA15 are plotted versus D_{rup}; A15 and observations are plotted versus R_{hypo}. The heavy solid line at the bottom of each panel shows $1/R$ trendline, plotted at an arbitrary amplitude level. (Left) Pseudospectral acceleration (PSA) at 1 Hz. (Right) PSA at 5 Hz. The color version of this figure is available only in the electronic edition.

of the ground-motion amplitudes. More detailed site corrections will require compilation of information on site conditions and/or empirical regressions to determine site terms. From Figure 6, we conclude that observations at distances < 15 km are generally consistent with the GMPEs, especially when one considers that none of these data were used in the GMPE derivations and that the conversions of observations to B/C conditions were not site-specific. A noteworthy observation is that the decay of amplitudes in the first 20 km appears to be quite steep, especially at high frequencies. The slope is steeper than the trend of $R_{hypo}^{-1.7}$ that applies to the A15 GMPE (at 5 Hz), and much steeper than the decay of $R_{hypo}^{-1.0}$ that is often assumed in ground-motion modeling. We emphasize the steepness of the distance scaling by plotting a line of slope $1/R$ for reference, at an arbitrary amplitude level, in Figure 6. The steep amplitude scaling with distance is apparent only at small-to-moderate magnitudes because for large magnitudes this effect is counteracted by an increasing near-distance saturation effect.

In Figure 7, we provide a fuller comparison of induced seismicity amplitudes to the predictions of the A15 GMPE by plotting residuals ($\log_{10}(\text{observed}) - \log_{10}(\text{predicted})$) for a selection of ground-motion parameters. The sole purpose is to illustrate how the data compare with the GMPE; a perfect match is neither expected nor achieved. A feature that is noted is a decreasing residual trend with distance at small magnitudes that appears to be countered by an increasing residual trend with distance at larger magnitudes. This may be a consequence of the magnitude-independent attenuation model assumed in the A15 GMPE. On the other hand, this apparent trend is not conclusive because the dataset does not extend uniformly to sufficiently large distances to enable the attenuation rates to be robustly defined. Larger databases (to hundreds of kilometers) are needed to adequately define attenuation trends; these will be determined in future studies. The A15 GMPE was not intended to be a good attenuation estimate at distances beyond 40 km, especially for CENA. The main point of Figure 7 is to illustrate that the A15 GMPE is a reasonable interim estimate of amplitudes for induced events. Because the YA15 CENA and ASK14 GMPEs are similar to A15, as shown previously, we may infer that these GMPEs are also applicable.

EPISTEMIC AND ALEATORY UNCERTAINTY IN INDUCED EVENT GMPES

Another important issue for hazard assessment for induced events concerns uncertainty in the GMPEs—both the epistemic

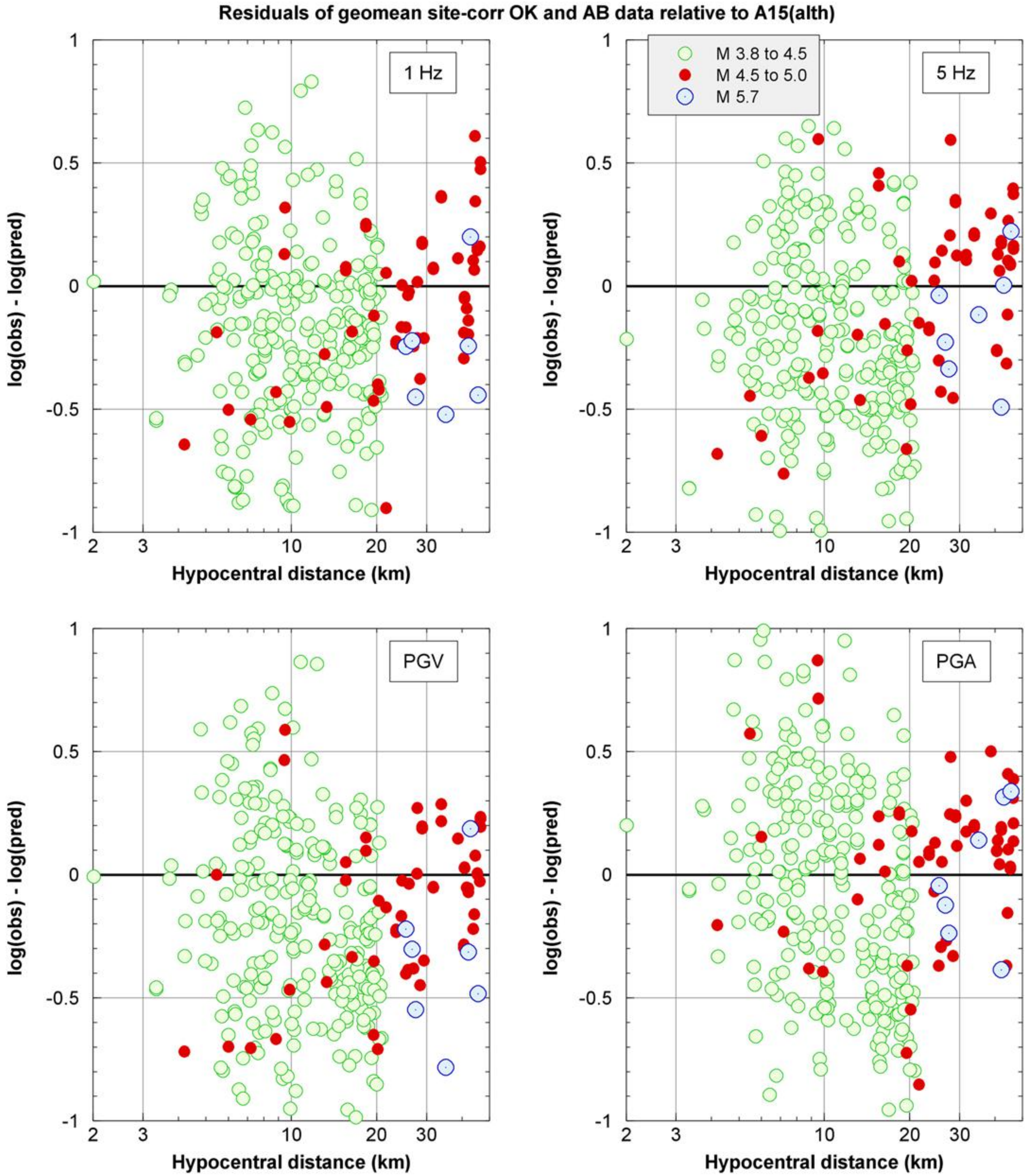

▲ **Figure 7.** Residuals (log_{10} units) for horizontal-component PSA at 1 and 5 Hz, peak ground velocity and peak ground acceleration for induced events in Oklahoma and Alberta, relative to the A15 (alternative-*h*) GMPE. Events of **M** 3.8–4.5 are compiled to 20 km; **M** ≥4.5 events are compiled to 50 km. The **M** 5.7 points are the 2011 Prague and 2016 Pawnee events. The color version of this figure is available only in the electronic edition.

uncertainty in the median prediction and the aleatory uncertainty (expressing scatter about the median). As for natural events, induced events have significant epistemic and aleatory uncertainty that can be attributed to variable source, path, and site effects. For induced-seismicity applications, the uncertainties in amplitudes at short epicentral distances are particularly complex and consequential. Moreover, the division of the uncertainty into its epistemic and aleatory components is challenging, especially for high-frequency ground motion, because we need to address the effects of focal depth on the stress parameter, as well as the random variability in stress parameter for a given depth and magnitude (see Fig. 5).

Considering variability in source parameters, the effect of focal depth could potentially be modeled as either an epistemic or aleatory uncertainty in a probabilistic seismic-hazard analysis (PSHA). In concept, this may be considered as an aleatory uncertainty, with depth being a random variable that is sampled from a focal depth distribution. In practice, however, depth is often modeled as an epistemic uncertainty within a logic-tree format for the sake of computational convenience in some PSHA software (e.g., Bommer and Scherbaum, 2008). In induced-seismicity GMPEs, the amplitude levels at high frequency will be particularly sensitive to this uncertainty and its treatment. A salient feature from Figure 5 that should be accommodated, which has both epistemic and aleatory components, is the high variability in stress parameter, even if the depth of the event is known. In practice, the depth is often not known in advance and thus is also uncertain.

The most important uncertainty in path effects is the attenuation at close distances, controlled by the near-source saturation term and the geometric spreading rate. All GMPEs shown in the comparison figure with ground-motion data from induced events (Fig. 6) feature similar near-distance saturation terms and have similar implied geometric spreading. Empirical data in both CENA and California show that steep attenuation ($R^{-1.3}$ in the first 50 km in the Fourier domain) is required to match the observed decay rate for small events, whereas for larger events there is a trade-off between the attenuation rate and the near-source saturation term (e.g., Yenier and Atkinson, 2014). The median value of the near-distance saturation term is constrained empirically (e.g., Atkinson *et al.*, 2016), but it also shows much variability, which maps into aleatory variability in amplitudes at close distances.

In considering the residuals plotted with respect to the A15 GMPE in Figure 7, the total variability is large at high frequencies. For example, the average of the PGA residuals is 0.00 ± 0.44 ($\log_{10}$ units). The standard deviation of 0.44 (a factor of 2.8) is significantly greater than the value of 0.37 (a factor of 2.3) that applies to the A15 GMPE (see Atkinson, 2015). The high variability likely reflects a number of factors, including the lack of site-specific conversions to B/C. Another factor influencing the variability, which is particularly relevant for induced seismicity applications, is that the A15 GMPE does not include focal depth as a predictive variable. We could potentially reduce ground-motion variability by including focal depth as a parameter, as in the YA15 CENA GMPE. However, if the focal depth is not known in advance, there would be no reduction in total variability, though we could recast some of the aleatory uncertainty into epistemic uncertainty. Thus, including focal depth as a predictive variable in induced-seismicity GMPEs may be useful for reduction in variability, but only if its value can be accurately predicted.

Figure 8 shows the mean event residual and its standard deviation for each of the events in the Assatourians and Atkinson (2017) database having five or more observations, and for all events (with as few as two observations) of $\mathbf{M} \geq 4.7$, with respect to the A15 GMPE. The within-event variability (noted by the error bars) is about $0.2 \log_{10}$ units on average. There is a suggestion that most events are overpredicted on average, but it should be kept in mind that this trend is distance dependent (Fig. 7) and may be driven by the more plentiful observations at larger distances. More detailed analysis of the components of both epistemic and aleatory uncertainty will require more complete datasets, as a codevelopment product of GMPE development.

CONCLUSIONS

There are few GMPEs derived directly from induced events in CENA in the magnitude–distance range of engineering interest, due to a lack of publicly available observational data. This is changing, and GMPEs will be developed at an increasing rate in the next few years. For example, there is a recent GMPE model that has been built using induced-seismicity data from the 2011 Prague, Oklahoma, sequence (Yenier *et al.*, 2017), though this development considered just a single highly productive event sequence. In the interim, GMPE models are needed for hazard assessments. Appropriate proxy GMPEs that are suitable for predicting motions from induced events in CENA may be selected from among published models having source and attenuation scaling attributes that make them suitable for the purpose. In this article, we have shown that the Abrahamson *et al.* (2014), Atkinson (2015), and Yenier and Atkinson (2015b) GMPEs are appropriate in functional form and overall amplitude level scaling. Note that an unspecified depth to top of rupture should be prescribed with ASK14 if it is to be used for this purpose. There may be other suitable GMPEs, because this article did not attempt to compile and evaluate a comprehensive list. The key attributes required of the GMPE include point-source near-distance scaling for small events and appropriate scaling of high-frequency amplitudes (stress parameter). Perhaps surprisingly, some GMPEs developed for natural earthquakes in California are applicable because of the fortuitous counterbalancing effects that focal depth and tectonic regime have on the stress parameter; this is why the A15 and ASK14 GMPEs, which were developed from the NGA-W2 database, appear to be very similar in their predictions to the YA15 CENA GMPE, which was developed from a simulation model calibrated to the NGA-E database.

In conclusion, the A15, YA15 (CENA), and ASK14 GMPEs all appear to be reasonable proxy estimates of median motions from moderate induced earthquakes in CENA at close distances. The aleatory and epistemic uncertainty in median

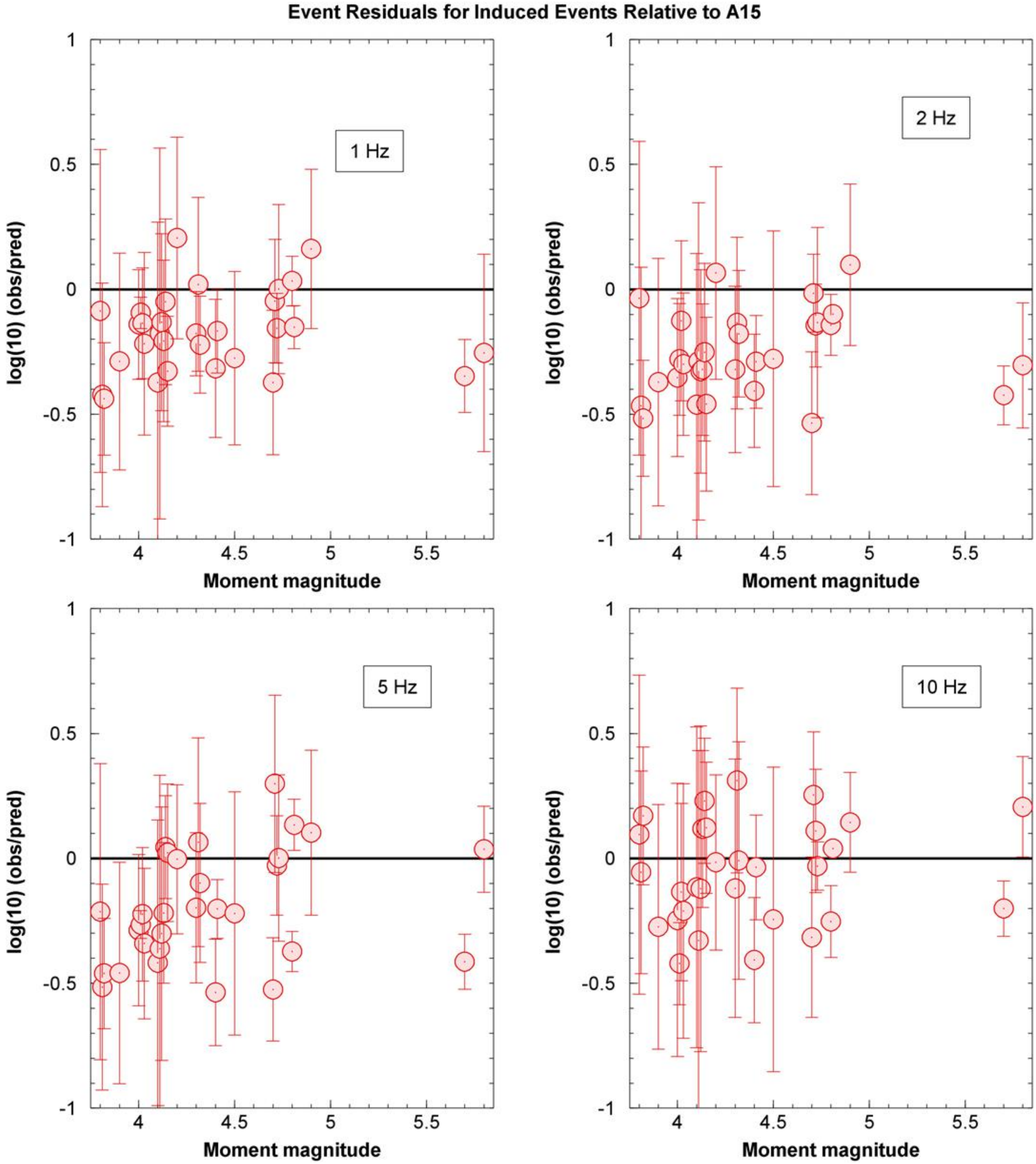

▲ **Figure 8.** Mean event residuals and standard deviation for the study events (Figs. 6 and 7) with respect to A15; residuals are plotted for events of **M** <4.7 with five or more observations, and for all events of **M** ≥4.7. Slight offsets (increments of 0.01 units) from actual **M** values are used for plotting clarity. The color version of this figure is available only in the electronic edition.

amplitudes for such events is at present larger than the corresponding values for natural earthquakes. Future work will develop GMPEs specifically for induced earthquakes in different environments, and investigate their uncertainty and variability.

DATA AND RESOURCES

Ground-motion amplitudes are from a database compiled from publicly available broadband and accelerometer recordings for events of **M** ≥ 3.8 recorded at close distances in Oklahoma and Alberta, processed as described by Assatourians and Atkinson (2010). Details of the records, processing, and time histories are provided in Assatourians and Atkinson (2017). The unpublished manuscript by K. Assatourians and G. Atkinson, "Development of a database of response spectra and time histories for induced earthquakes," has been submitted to *Seismol. Res. Lett.* Most of the data may be downloaded directly from Incorporated Research Institutes for Seismology. Ground-motion data for California (Fig. 3) are from Atkinson (2015). Ground motions for the Next Generation Attenuation (NGA)-West2 ground-motion prediction equations were evaluated using a spreadsheet available at www.peer.berkeley.edu (last accessed August 2016). Details of the NGA-East and NGA-West2 database compilations are provided at www.peer.berkeley.edu (last accessed November 2016).

ACKNOWLEDGMENTS

The financial support of the Natural Sciences and Engineering Research Council is gratefully acknowledged. We are grateful to Chris Cramer, Martin Chapman, and an anonymous reviewer for insightful and constructive comments that improved the article.

REFERENCES

Abrahamson, N. A., W. J. Silva, and R. Kamai (2014). Summary of the Abrahamson, Silva, and Kamai NGA-West2 ground-motion relations for active crustal regions, *Earthq. Spectra* **30,** 1025–1056.

Assatourians, K., and G. Atkinson (2010). Database of processed time series and response spectra for Canada: An example application to study of the 2005 MN5.4 Riviere du Loup, Quebec earthquake, *Seismol. Res. Lett.* **81,** 1013–1031.

Atkinson, G. (2015). Ground-motion prediction equation for small-to-moderate events at short hypocentral distances, with application to induced seismicity hazards, *Bull. Seismol. Soc. Am.* **105,** doi: 10.1785/0120140142.

Atkinson, G., H. Ghofrani, and K. Assatourians (2015). Impact of induced seismicity on the evaluation of seismic hazard: Some preliminary considerations, *Seismol. Res. Lett.* **86,** 1009–1021.

Atkinson, G., E. Yenier, N. Sharma, and V. Convertito (2016). Constraints on the near-distance saturation of ground-motion amplitudes for small-to-moderate induced earthquakes, *Bull. Seismol. Soc. Am.* **106,** doi: 10.1785/0120160075.

Bommer, J., and F. Scherbaum (2008). The use and misuse of logic trees in probabilistic seismic hazard analysis, *Earthq. Spectra* **24,** 997–1009.

Boore, D. (2003). Prediction of ground motion using the stochastic method, *Pure Appl. Geophys.* **160,** 635–676.

Boore, D., J. Stewart, E. Seyhan, and G. Atkinson (2014). NGA-West2 equations for predicting PGA, PGV, and 5% damped PSA for shallow crustal earthquakes, *Earthq. Spectra* **30,** no. 3, 1057–1085.

Bourne, S., S. Oates, J. Bommer, B. Dost, J. van Elk, and D. Doornhof (2015). A Monte Carlo method for probabilistic hazard assessment of induced seismicity due to conventional natural gas production, *Bull. Seismol. Soc. Am.* **105,** 1721–1738.

Campbell, K. W., and Y. Bozorgnia (2014). Campbell-Bozorgnia NGA-West2 ground motion model for the average horizontal components of PGA, PGV, and 5%-damped linear response spectra, *Earthq. Spectra* **30,** 1087–1116.

Chiou, B. S. J., and R. Youngs (2014). Update of the Chiou and Youngs NGA ground motion model for average horizontal component of peak ground motion and response spectra, *Earthq. Spectra* **30,** 1117–1154.

Kanamori, H., and D. Anderson (1975). Theoretical basis of some empirical relations in seismology, *Bull. Seismol. Soc. Am.* **65,** 1073–1095.

Seyhan, E., and J. Stewart (2014). Semi-empirical nonlinear site amplification from NGA-West2 data and simulations, *Earthq. Spectra* **30,** 1241–1256.

Yenier, E., and G. Atkinson (2014). Point-source modeling of moderate-to-large magnitude earthquakes and associated ground-motion saturation effects, *Bull. Seismol. Soc. Am.* **104,** 1458–1478, doi: 10.1785/0120130147.

Yenier, E., and G. Atkinson (2015a). An equivalent point-source model for stochastic simulation of earthquake ground motions in California, *Bull. Seismol. Soc. Am.* **105,** 1435–1455.

Yenier, E., and G. Atkinson (2015b). A regionally-adjustable generic GMPE based on stochastic point-source simulations, *Bull. Seismol. Soc. Am.* **105,** 1989–2009.

Yenier, E., G. M. Atkinson, and D. F. Sumy (2017). Ground motions for induced earthquakes in Oklahoma, *Bull. Seismol. Soc. Am.* **107,** no. 1, doi: 10.1785/0120160114.

Gail M. Atkinson
Karen Assatourians
Department of Earth Sciences
Western University
London, Ontario
Canada N6A 5B7
gmatkinson@aol.com

Published Online 1 February 2017